Anal Bioanal Chem (2012) 402:3237–3244
DOI 10.1007/s00216-012-5771-7

ORIGINAL PAPER

A photosynthetic biosensor with enhanced electron transfer generation realized by laser printing technology

Eleftherios Touloupakis · Christos Boutopoulos · Katia Buonasera · Ioanna Zergioti · Maria Teresa Giardi

Received: 30 November 2011 / Revised: 16 January 2012 / Accepted: 18 January 2012 / Published online: 3 February 2012

Abstract One of the limits of current electrochemical biosensors is a lack of methods providing stable and highly efficient junctions between biomaterial and solid-state devices. This paper shows how laser-induced forward transfer (LIFT) can enable efficient electron transfer from photosynthetic biomaterial immobilized on screen-printed electrodes (SPE). The ideal pattern, in terms of photocurrent signal of thylakoid droplets giving a stable response signal with a current intensity of approximately 335±13 nA for a thylakoid mass of 28±4 ng, was selected. It is shown that the efficiency of energy production of a photosynthetic system can be strongly enhanced by the LIFT process, as demonstrated by use of the technique to construct an efficient and sensitive photosynthesis-based biosensor for detecting herbicides at nanomolar concentrations.

Keywords Laser printing · Biosensor · Photosynthesis · Herbicides

Published in the topical collection *Biomimetic Recognition Elements for Sensing Applications* with guest editor María Cruz Moreno-Bondi.

E. Touloupakis · K. Buonasera · M. T. Giardi
Institute of Crystallography, National Research Council,
Via Salaria Km 29.300, Monterotondo Scalo,
00015 Rome, Italy

E. Touloupakis (✉)
Biosensor srl,
Via degli Olmetti 44, Formello,
00060 Rome, Italy
e-mail: toulou_e@chemistry.uoc.gr

C. Boutopoulos · I. Zergioti
Department of Physics, National Technical University of Athens,
Iroon Polytehneiou 9, Zografou,
15780 Athens, Greece

Introduction

Use of biosensors is becoming fairly widespread throughout the world. Since the first studies on early prototypes, much progress has been made in biosensor technology and nowadays these devices are easy, quick, and inexpensive solutions to many different analytical problems [1]. This success is a result of the combination of multidisciplinary competence which has enabled perfect integration of chemistry, biology, and electronics in single, portable, and easy to use instruments. Because of these features, integration of biological material into a device is being regarded as appropriate for many future fields of analysis, and seems particularly suitable for those in which large numbers of samples must be collected and analyzed daily to perform water or food-monitoring programs.

Despite their clear advantages, however, there are still technical concerns in biomimetics which challenge researchers. One of the main problems is achieving stable, integral junctions between the biorecognition element (also called the "biomediator") and the transduction system. Realization of such junctions in a sensor is essential for efficient conversion of a biochemical signal into an electrical signal [2].

Plants, algae, and cyanobacteria used the electron-transfer chain of the photosynthetic process to synthesize ATP molecules needed for metabolic reactions. The electron-transfer chain starts in the photosynthetic reaction center of photosystem II (PSII), a light-driven water–plastoquinone oxidoreductase which catalyzes the most thermodynamically demanding reaction in biology. This multi-enzymatic complex is embedded in thylakoid membranes, and is composed of two proteins, D1 and D2, which contain all the cofactors necessary for photochemical charge separation [3]. On illumination, the excited primary electron donor, P680*, ejects an electron into the final electron acceptor, the plastoquinone Q_B, via

chlorophyll, pheophytin, and plastoquinone Q_A [4, 5]. Whereas Q_A is fixed within the structure, Q_B is, in vivo, released into the membrane matrix after accepting two electrons and undergoing protonation. Several compounds used as herbicides compete with plastoquinone in the Q_B site, blocking this electron transfer in a concentration-dependent manner; for this reason, photosynthetic organisms and organelles containing PSII have been extensively considered for construction of photosynthesis-based biosensors [6–13].

Several papers have been published on assembly of photosynthetic biosensors by immobilization of intact cells, thylakoid membranes, and core complexes on screen-printed electrodes [14–20]. Most of these were designed to measure either changes in photocurrent [17, 21] or inhibition of electron transport by artificial mediators [14, 15, 18, 22]. A variety of immobilization techniques have been developed to improve both physical and chemical contact between the biological material and the electrodes [23]. Those most commonly used are cross-linking in a bovine serum albumin–glutaraldehyde matrix, in poly(vinyl alcohol), or in calcium alginate gels [14, 16, 23, 24]. These techniques have several disadvantages, for example denaturation of the biomaterial and use of toxic reagents, and they often interfere with, or attenuate, the signal of the analyte.

To overcome the limits of previously evaluated immobilization techniques, a new technique, denoted "laser-induced forward transfer" or "LIFT", has been considered in this work. The objective was to ensure rapid, non-destructive integration of biological material into solid-state devices. The LIFT technique consists in irradiating, by use of a pulsed laser, a thin layer of an absorbing material previously deposited on to a transparent substrate. The layer is irradiated through the substrate and the light–matter interaction which occurs at the interface generates a large increase of local pressure. As a result, a small piece of the material located in front of the irradiated area is immediately ejected from the substrate surface and deposited on to a target substrate arranged to be in close proximity. The LIFT technique, previously tested on many varieties of biomaterial (proteins [25, 26], DNA [27, 28], living cells [29], and thylakoids [30]), has been used here to create a new photosynthetic biosensor in which thylakoids are stably and efficiently bound to the transducer, even under the measurement conditions. It is shown that the highly energetic transfer of the thylakoids cause by the LIFT process forces the biomaterial into the porous electrode structure, and thus greatly enhances physical adsorption, promoting electron transfer to the electrode.

Compared with the whole cells of photosynthetic microrganisms, thylakoids have the advantage of giving better current signals, because of the smaller number of membranes to be crossed during electron transport; for this reason they have been considered in this study. The results obtained demonstrated that use of biomediators in highly efficient immobilization techniques enables successful construction of new-generation photoelectrochemical devices, which could be useful for transmission, storage, or direct usage of the natural electron flow into solid-state devices, for example photodetectors and photovoltaic cells.

Materials and methods

Disposable screen-printed electrodes, gold (C223BT), carbon paste (DRP110), and multi-walled carbon nanotubes (DRP110CNT) were purchased from DropSens (Oviedo, Spain). All reagents in this study were of analytical grade and purchased from Sigma–Aldrich (St Louis, MO USA).

Thylakoid membrane preparation

To isolate thylakoid membranes from fresh spinach leaves (*Spinacea oleracea* L.), leaves (100 g) were washed with deionized water, dried on filter paper, and homogenized in 300 mL extraction buffer containing *N*-(2-hydroxy-1,1-bis (hydroxymethyl)ethyl)glycine (tricine) 20 mmol L^{-1} pH 7.8, $MgCl_2$ 5 mmol L^{-1}, sucrose 0.3 mol L^{-1}, bovine serum albumin 2% *w*/*v* and ethylenediaminetetraacetic acid 1 mmol L^{-1}. The homogenate was filtered through two layers of miracloth and centrifuged for 2 min at 700*g*. The supernatant was centrifuged at 7500*g* for 10 min and the resulting pellet was re-suspended in the re-suspending buffer containing 2-(*N*-morpholino)ethanesulfonic acid (MES) pH 6.0, sucrose 70 mmol L^{-1}, and NaCl 15 mmol L^{-1}. The new pellet was stirred again in the re-suspending buffer and centrifuged at 7500*g* for 10 min to obtain thylakoid membranes. Aliquots were placed in Eppendorf tubes and kept at −80 °C. All steps were performed at 4 °C in the dark.

Photosynthetic material characterization

Chlorophyll content was calculated in accordance with Porra [31] by use of the formulas:

$$\begin{aligned}\text{Total chlorophyll} &= [(A_{645} \times 20.2) + (A_{663} \times 8.02)]/5 \times \text{dilution}\\ [\text{Chl}\alpha] &= 12.25 \times A_{663.6} - 2.55 \times A_{646.6}\\ [\text{Chl}\beta] &= 20.31 \times A_{646.6} - 2.55 \times A_{663.6}\end{aligned}$$

The stability of the photosynthetic material before immobilization was tested by measuring changes in fluorescence yield with 650 nm light excitation after 10 min of dark adaptation. Isolated thylakoid membranes were tested by use of a Plant Efficiency Analyser (Hansatech Instruments, UK) at room temperature. The maximum fluorescence yield from photosynthetic membranes was generated by using six

red high-intensity light-emitting diodes (LEDs) (broad band 650 nm). The light pulse duration was 2 s.

LIFT of thylakoid membranes

Deposition of thylakoid membranes on to the working gold electrode was achieved by use of the experimental apparatus depicted in Fig. 1 and using a pulsed Nd:YAG (yttrium aluminium garnet) laser (266 nm wavelength, 4 ns pulse duration) with a high-power imaging micromachining system, described in detail elsewhere [32, 33].

The donor substrates were prepared by drop casting 10 μL thylakoid solution on to 1-in quartz plates coated with a 40-nm titanium laser-absorbing layer. The final concentration of the thylakoid solution on the target substrate was 7.6 mg mL^{-1}. Two-dimensional patterns of discrete thylakoid droplets and continuous thylakoid layers were printed on the electrodes by adjusting the droplet-separation distance as described elsewhere [30]. The transfer was performed in such a way that each droplet was deposited by a single pulse; the optimum distance between the donor and the substrate was found to be 300 μm. After the optimization study, laser transfer was performed at 470 mJ cm^{-2} and the laser beam size on the donor substrate was 60 μm in diameter. By using these laser conditions the deposited thylakoid droplets on the electrode surface were 150 μm in diameter.

SEM analyses

A field emission FEI NovaSEM 230A system with attached Everhard–Thornley detector (ETD) was used for SEM observations. SEM images were taken in high-vacuum mode with an electron accelerating voltage of 2 kV. After LIFT immobilization of the thylakoids on the central working electrode, SPEs were cut into two pieces and covered with a thin gold layer (~5 nm) by sputtering. Cross-section SEM images were then obtained to investigate the attachment of the thylakoids to the electrode surface.

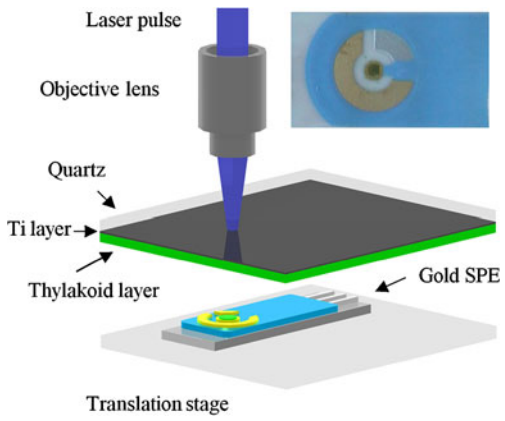

Fig. 1 Schematic illustration of the LIFT process. The *inset* shows a gold SPE. The central working electrode is coated with a continuous layer of thylakoid solution printed by use of LIFT

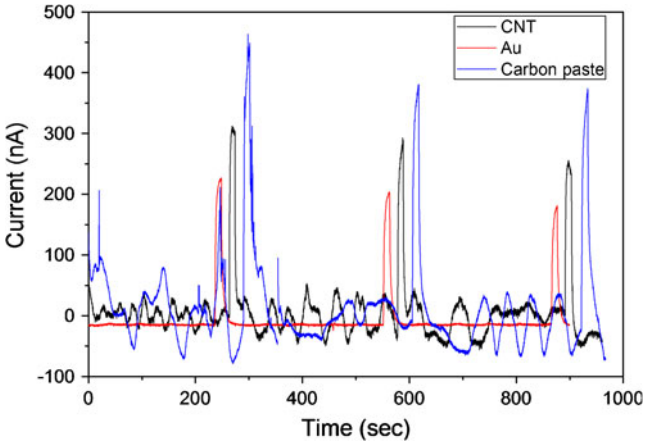

Fig. 2 Chronoamperometric signals produced by thylakoid membranes immobilized by the LIFT technique on three different types of SPE (response times were intentionally shifted for better visualization)

Biosensor set-up

Tests with the immobilized photosynthetic material on the SPEs were performed by use of the Ampbiospe system (Biosensor, Rome, Italy; www.biosensor.it), which contains a polyoxymethylene flow cell and the PG580 potentiostat (Uniscan Instruments, UK). The SPEs, with the immobilized photosynthetic material, were mounted in the flow cell (volume 50 μL) which was equipped with two light-emitting diodes and polarized at +0.2 V relative to an Ag/AgCl reference electrode.

Amperometric detection of the electric current generated by the thylakoid membranes was measured after illumination by two red LEDs (peak wavelength 652 nm, with light intensity 130 μmol photons m^{-2} s^{-1}) for 7 s in the presence of the artificial electron acceptor 2,6-dichlorophenol–indophenol (DCPIP). The electrode was continuously washed with measurement buffer containing tricine 20 mmol L^{-1} pH 7.8, sucrose 70 mmol L^{-1}, NaCl 15 mmol L^{-1}, $MgCl_2$ 5 mmol L^{-1}, and DCPIP 30 μmol L^{-1} at a flow rate of 130 μL min^{-1}.

Table 1 Chronoamperometric signal intensity and calculated mass of thylakoid droplets spotted on to Au SPEs. The photocurrent signal error is the standard deviation for four inter-electrode measurements

Number of spots	Signal (nA)	Thylakoids (ng)
36	180.3±5.5	5.3±0.8
64	220.5±21.0	9.4±1.4
100	233.2±9.5	14.6±2.2
132	273.9±12.5	19.3±2.9
196	335.2±13.4	28.7±4.3
256	326.0±16.2	37.5±5.6

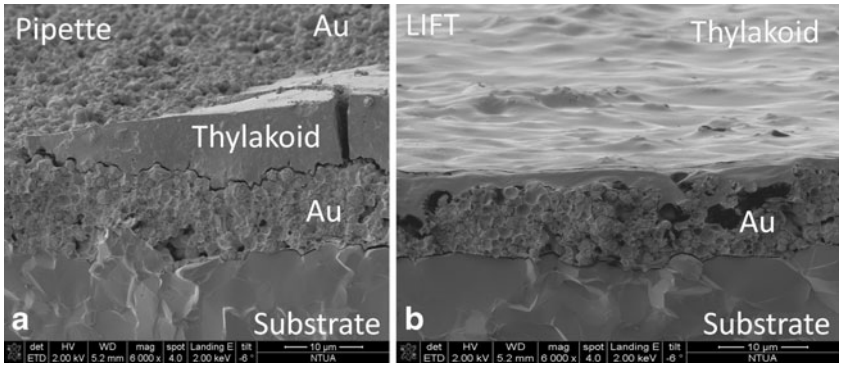

Fig. 3 Cross-section SEM images of the Au working electrode printed with thylakoid membranes by use of: **a**) the reference pipette method, **b**) laser-induced forward transfer. Images were obtained before the flow conditions measurement step

The inhibitory effect of herbicides on the photosynthetic activity was evaluated by recording the current due to re-oxidation of the reduced form of the artificial electron acceptor DCPIP, which was formed during the photosynthetic step. When the system was illuminated, the photosynthetic reaction occurred, releasing oxygen and reducing the electron acceptor present in the measurement buffer. This was then re-oxidized at the electrode surface by applying a suitable potential (+0.2 V), and a current peak proportional to the photosynthetic activity was recorded.

The principle of herbicide detection is based on the decrease of the rate of electron transport in the biosensor signal. First, the activity in the absence of herbicide was recorded. The herbicide-containing sample was then loaded into the flow cell and the residual activity was recorded. The herbicide was then removed by use of measurement buffer and the biosensor used for a new analysis. Each herbicide concentration was used in 3–5 independent measurements. All measurements were performed at 25.0±0.1 °C.

Results and discussion

Thylakoid membranes tethered to screen-printed electrodes by the laser-induced technique

In intact photosynthetic cells oxygen evolution reflects the photolysis of the water in PSII and is associated with non-cyclic flow of electrons from the water to $NADP^+$ and, ultimately, to 3-phosphoglyceric acid. These factors are lost during isolation of the chloroplasts, but artificial mediators, for example potassium ferricyanide (FeCy) or DCPIP, can be used as substitute electron acceptors [18]. Thus, the rate of the electron transfer measured by reduction of artificial electron acceptors is a measure of photosynthetic activity.

Under illumination the active photosynthetic membranes are able to transfer electrons to the DCPIP. The reduced form of DCPIP is electrochemically reoxidized at the specific applied potential (+0.2 V), generating an electric current. The rate of photosynthetic electron transfer measured by reduction of the artificial mediator reflects photosynthetic activity.

Different conditions and properties were tested to assess the immobilization procedure in relation to biological material and operational stability. The conditions were two-dimensional patterns, spot dimensions, different screen printed electrode substrates, laser energy, and beam size. The current signal and the signal to noise ratio (*S*/*N*) depend on many experimental factors, for example chlorophyll content, composition of the buffer used for the measurements, and the surface properties of interface between the immobilized cells and the SPE, etc.

First, laser-printing experiments were performed on three different types of SPE, carbon paste (CP), gold (Au), and multi-walled carbon nanotubes (CNT), to chose the support with the best performance. For these experiments a

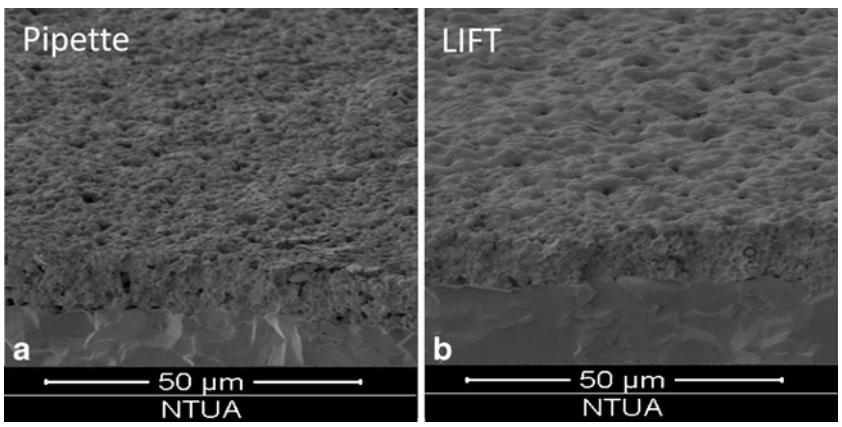

Fig. 4 Cross section SEM images of the Au working electrode printed with thylakoid membranes by use of: **a**) the reference pipette method, **b**) laser induced forward transfer. Images were obtained after the flow conditions measurement step

preliminary pattern containing 64 spots was considered. After the printing, the bioactivity of the thylakoid transferred material was evaluated as photocurrent signals. Photocurrent signals were measured in a flow-cell system under the experimental conditions described in the section "Biosensor set-up".

As is apparent from the chronoamperometric diagram in Fig. 2, the thylakoids printed on gold SPE had the lowest photocurrent signal (242 nA compared with 460 nA for CP and 327 nA for CNT electrodes). However, the gold SPEs had the best signal-to-noise ratio with $S_1/N_1=40.3>S_2/N_2=3.5>S_3/N_3=2.9$, where S is the current signal produced and N the noise (1 for gold, 2 for CP, and 3 for the CNT SPE) and a very stable baseline (Fig. 2). These differences can be explained by the irregular structure and the presence of undefined reactive functional groups of the CP and the CNT, the different resistivity, and the different contact resistances of the three types of electrode. As a result of this study further printing experiments were focused on gold SPEs.

Different two-dimensional patterns of thylakoid droplets were printed on the gold working electrode's surface and tested for photosynthetic activity. Printing of thylakoid material was carried out in such a way that an array of material droplets (6×6=36 droplets, 8×8=64 droplets etc.) covered a 1 mm×1 mm area on the working electrode. The arrays of droplets were printed by increasing the numbers of spots and adjusting the distance between them to cover a 1 mm× 1 mm area. This methodology eliminates the undesirable "coffee ring" effect and ensures uniform coverage of the working electrode by the thylakoid material [34]. Deposition of 100 droplets was the limit to form a continuous layer on the electrode (Fig. 1, inset). Selection of fewer droplets resulted in the formation of discrete droplets on the electrode instead of a continuous layer. As can be seen in

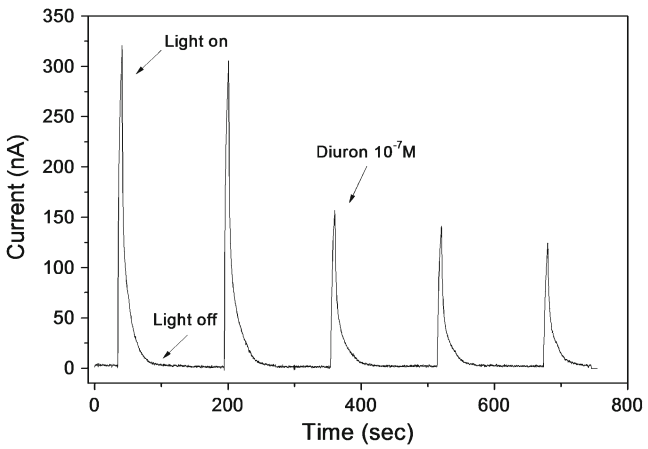

Fig. 5 Photocurrent changes of the photosynthetic biosensor in response to switching of light (7 s illumination followed by 150 s in the dark) and addition of diuron herbicide (10^{-7} mol L^{-1}). The photosynthetic material was illuminated twice before addition of the herbicide

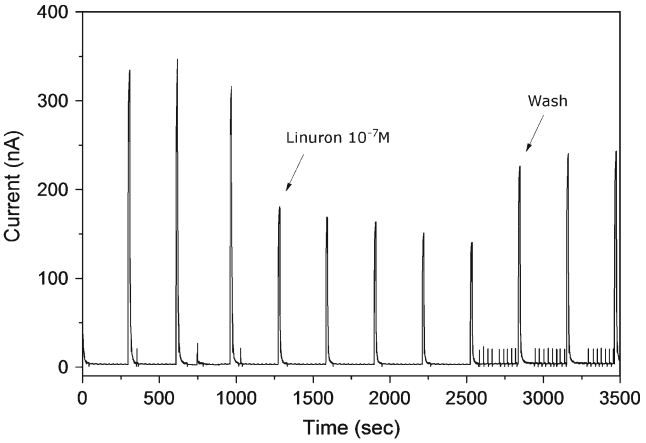

Fig. 6 Regeneration of the photosynthetic biosensor by washing with buffer after typical analysis of linuron (10^{-7} mol L^{-1})

Table 1, for the first five patterns the photocurrent response increases with increasing the number of spots. The ideal pattern in terms of photocurrent signal is that of 196 spots. This pattern gives a stable response signal with current intensity of 335.2±13.4 nA, the calculated thylakoid mass corresponds to 28.7±4.3 ng. Thus, the pattern of 196 spots was chosen for immobilization of the photosynthetic material and for development of the biosensor. Further increasing the number of spots resulted in a slight decrease of the photocurrent signal combined with a slight decrease of the signal-to-noise ratio.

SEM results

Direct LIFT immobilization of the thylakoids on the SPEs occurs because of the high-kinetic-energy transfer of the material. After laser irradiation of the donor substrate, the thylakoid material is transferred to the SPE electrode by high-velocity jet formation (~100 ms^{-1}) [35]. As a result, a high impact pressure of few MPa is induced at the rough electrode surface [36]. The combination of high impact pressure and the high-roughness electrode surface (rms 1.5 μm), leads to a complete wetting state that enhances physical adsorption of the thylakoid membranes. Recently, we have shown that this immobilization process could not be reproduced by conventional spotting methods, for

Table 2 Calculated LOD, relative standard deviation (RSD), and I_{50} values for the herbicides diuron and linuron

Herbicide	I_{50} (mol L^{-1})	RSD (%)	LOD (mol L^{-1})[a]	LOD (mol L^{-1})[b]
Diuron	1.87×10^{-7}	2.59	1.3×10^{-8}	8.0×10^{-9}
Linuron	5.65×10^{-8}	2.07	3.1×10^{-9}	4.0×10^{-9}

[a] In accordance with Malya et al. [38]

[b] In accordance with IUPAC recommendation

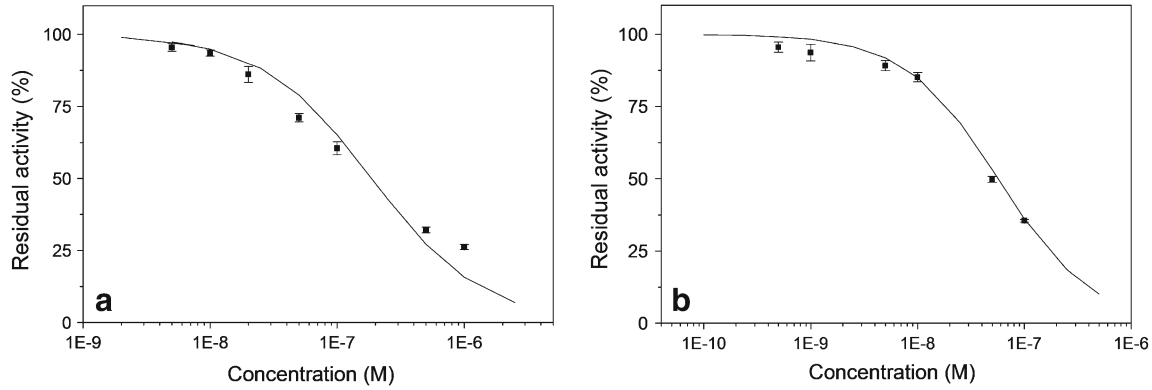

Fig. 7 Calibration curves for the herbicides diuron (**a**) and linuron (**b**). The residual activity (%) was calculated as the ratio of signals in the presence/absence of the herbicide

example pipetting [30]. SEM analysis was conducted to further investigate the phenomenon. Cross-section images of the central working electrode were taken before and after the measurement step for both LIFT and pipette-printed gold SPEs. Figure 3a shows a cross-section SEM image of a gold working electrode covered by a thylakoid layer using the reference pipette method. Characteristic cracks can be observed at the thylakoid layer–electrode surface interface. In contrast, LIFT immobilization resulted in the formation of a uniform thylakoid layer on the electrode that penetrates the porous rough surface (Fig. 3b). The corresponding SEM images after the measurement step for pipette spotting and LIFT are shown in Fig. 4a, b, respectively. After pipette deposition the thylakoid layer has been totally removed from the electrode surface. In contrast, after LIFT immobilization, a thin uniform thylakoid layer remains on the electrode, ensuring high photocurrent activity. The thylakoid layer was measured, by use of a profilometer, to have an average thickness of approximately 1 μm.

Sensor performance

The principle exploited by this biosensor was light-induced activation of the electron transport chain, from the PSII of thylakoids to the SPEs. This process, which mimics the natural transfer occurring from the PSII reaction centers of plants, algae, and cyanobacteria to the plastoquinone Q_B involved in the first stage of photosynthesis, is partially or totally blocked in presence of photosynthetic herbicides, and can be therefore used to reveal traces of herbicides [37].

Inhibition of the activity of the immobilized photosynthetic material was tested in the presence of different concentrations of the herbicides linuron (3-(3,4-dichlorophenyl)-1-methoxy-1-methylurea) and diuron (3-(3,4-dichlorophenyl)-1,1-dimethylurea). Amperometric detection of the electric current generated by thylakoid membranes was measured after 7 s of illumination by the two LEDs (peak wavelength 652 nm, with light intensity 130 μmol photons m^{-2} s^{-1}) in the presence of DCPIP. As already stated, DCPIP is the most commonly used artificial electron acceptor, and can accept electrons instead of the pool of plastoquinones. Because electron flow through PSII is affected by the presence of herbicides, the reduction of DCPIP is proportional to herbicide concentration. The principle of detection is based on the fact that herbicides selectively block electron-transport activity in a concentration-dependent manner. Changes of the activity were recorded amperometrically as rate of photoreduction of the artificial electron acceptor.

Initially, the activity of the immobilized photosynthetic material was recorded in the absence of the herbicides, then the photosynthetic material was washed with 4 mL herbicide solution and the residual activity was recorded again (Fig. 5). The ratio between these two measurements was determined. All tests reported in this work were carried out on freshly prepared SPE. Used SPEs could be regenerated by washing away the herbicide solution with measurement buffer. A typical analysis followed by regeneration of the sample is

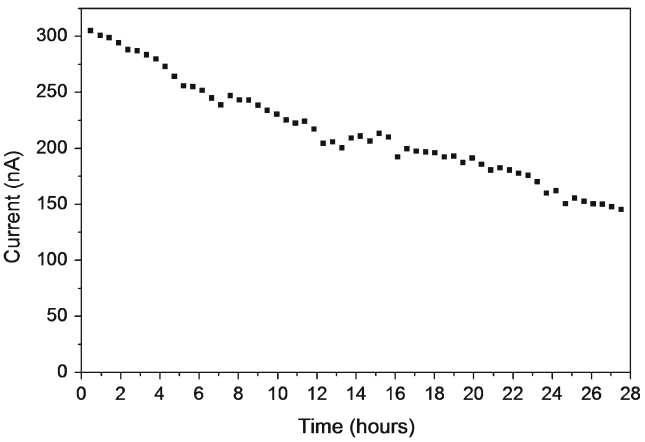

Fig. 8 Continuous measurements of electron transfer of spinach thylakoids immobilized by LIFT on printed electrodes

depicted in Fig. 6. After use of linuron (10^{-7} mol L^{-1}) percentage recovery after one wash was ~80%. This value is equal to that reported by Touloupakis et al. [14].

Response curves for each herbicide were analyzed by use of the Langmuir adsorption isotherm:

$$\text{act} = 100 - 100 \times [\text{H}]/(\text{I50} + [\text{H}])$$

where act is the residual activity of the biosensor (%) after addition of the herbicide, where [H] is the concentration of herbicide in the solution, and I_{50} is the herbicide concentration causing a 50% inhibition of the activity. Calculation of the detection limit (LOD) was based on a 99% confidence interval, which, assuming the normal distribution, corresponds to 2.6 × the relative standard error of the measurement (σ). By use of the modified relationship for the Langmuir adsorption isotherm the LOD was calculated as:

$$\text{LOD} = 2.6 \times \sigma \times I_{50}/(100 - 2.6 \times \sigma)$$

[38]

The LOD was also calculated in accordance with IUPAC recommendations [39]. The I_{50} values for the two herbicides and their detection limits are listed in Table 2. The calibration curves are depicted in Fig. 7.

The set-up resulted in an herbicide sensor with a half life of 24 h (Fig. 8). The stability of the biosensor was tested under continuous flow conditions (200 μL mL^{-1}) at room temperature. Immobilized electrodes stored at −20 °C maintained their performance for at least three months.

This sensor uses very low quantities of the photosynthetic material, up to 30 ng, compared with the several micrograms used in previous photosynthetic biosensors [14, 15, 18, 38]. The sensor had a high photocurrent signal with an excellent signal-to-noise ratio. The signal, approximately 330 nA, was much higher than the signal reported in previous work [14, 18, 20]. It should be noted that this value is produced by an amount of photosynthetic material at least a factor of 35 less than in the other sensors. The biosensor was able to detect photosynthetic herbicides of the ureic class in a short time with detection limits in the nanomolar range. The detection limit is in accordance with the maximum admissible concentration imposed by European Community norms, 0.1 μg L^{-1} (for each single pollutant) and 0.5 μg L^{-1} (for total herbicides).

Conclusions

Appropriate combination of biological molecules, supramolecules, and living cells with artificial supports has proved to lead to systems with enhanced performance compared with isolated biological matter. The hybrid materials can be used in diverse applications in which immobilized photosynthetic structures can be used. The main problem is efficient capture of the energy produced by photosynthetic organisms. In phototransport experiments with photosynthetic thylakoids, we showed that the laser-induced forward transfer (LIFT) technique can enhance energy conversion in electrochemical sensors.

By use of the LIFT technique, thylakoid membranes were interfaced with SPEs of different material (gold, carbon paste, and carbon-nanotubes), to select the best in terms of current yield. The technique seemed particularly suitable for deposition on gold SPEs, resulting in a valid alternative to those methods in which the photosynthetically active material must be covalently bonded to be highly efficiently interfaced with Au electrodes [40, 41]. Moreover, the LIFT technique enables high-spatial-resolution printing of liquid biomaterials. Printing resolution of few microns could be achieved, which makes the technique ideal for depositing biomaterial on microelectrode sensing devices.

This photosynthesis-based biosensor has revealed that the LIFT technique can establish efficient electrochemical contact between proteins and electrode, stabilizing the photosynthetic biomolecule and transporting electrons with high efficiency. The great advantage of using LIFT as a mild physical method is that it enables the biological material to be interfaced with solid substrates without damaging the biomaterial itself or its vital functions, while creating extremely solid junctions with the electrodes.

Acknowledgements The work discussed in this paper used technology developed in projects with financial support from the European Commission (e-LIFT FP7 ICT, grant agreement no. 247868; BEEP-C-EN FP 7-SME-2008-01, grant agreement no. 231082, SENSBIOSYN FP 7-SME-2008-01, grant agreement no. 232522), which is gratefully acknowledged.

References

1. Luong JHT, Male KB, Glennon JD (2008) Biosensor technology: technology push versus market pull. Biotechnol Adv 26(5):492–500
2. Rodriguez-Mozaz S, Lopez de Alda MJ, Barceló D (2006) Biosensors as useful tools for environmental analysis and monitoring. Anal Bioanal Chem 386:1025–1041
3. Giardi MT, Pace E (2005) Photosynthetic proteins for technological applications. Trends Biotechnol 23(5):257–263
4. Gant E (1996) Pigment protein complexes and the concept of the photosynthetic unit: chlorophyll complexes and phycobilisomes. Photosynth Res 48:47–53
5. Guskov A, Kern J, Gabdulkhakov A, Broser M, Zouni A, Saenger W (2009) Cyanobacterial photosystem II at 2.9 Å resolution and the role of quinones, lipids, channels and chloride. Nat Struct Mol Biol 16:334–342
6. Oettmeier W (2003) In: Plimmer JR (ed) Encyclopedia of agrochemicals vol. 2. John Wiley & Sons, Inc, Hoboken
7. Ackerman F (2007) The economics of atrazine. Int J Occup Environ Health 13:441–449

8. Shitanda I, Takamatsu S, Watanabe K, Itagaki M (2009) Amperometric screen-printed algal biosensor with flow injection analysis system for detection of environmental toxic compounds. Electrochim Acta 54:4933–4936
9. Li J, Wei X, Peng T (2005) Fabrication of herbicide biosensors based on the inhibition of enzyme activity that catalyzes the scavenging of hydrogen peroxide in a thylakoid membrane. Anal Sci 21:1217–1222
10. Rouillon R, Boucher N, Gingras Y, Carpentier R (2000) Immobilization of photosystem II submembrane fractions in poly(vinylalcohol) bearing styrylpyridium groups. Application to the detection of heavy metals. J Chem Technol Biotechnol 75:1003–1007
11. Rodriquez M, Sanders CA, Greenbaum E (2002) Biosensors for rapid monitoring of primary-source drinking water using naturally occurring photosynthesis. Biosens Bioelectron 17:843–849
12. Podola B, Melkonian M (2003) A long-term operating algal biosensor for the rapid detection of volatile toxic compounds. J Appl Phycol 15:415–424
13. Moreno-Garrido I (2008) Microalgae immobilization: current techniques and uses. Bioresour Technol 99:3949–3964
14. Touloupakis E, Giannoudi L, Piletsky SA, Guzzella L, Pozzoni F, Giardi MT (2005) A multi-biosensor based on immobilized photosystem II on screen-printed electrodes for the detection of herbicides in river water. Biosens Bioelectron 20:1984–1992
15. Bettazzi F, Laschi S, Mascini M (2007) One-shot screen-printed thylakoid membrane-based biosensor for the detection of photosynthetic inhibitors in discrete samples. Anal Chim Acta 589:14–21
16. Campàs M, Carpentier R, Rouillon R (2008) Plant tissue-and photosynthesis-based biosensors. Biotechnol Adv 26(4):370–378
17. Avramescu A, Rouillon R, Carpentier R (1999) Potential for use of a cyanobacterium *Synechocystis* sp. immobilized in poly(vinylalcohol): application to the detection of pollutants. Biotechnol Tech 13:559–562
18. Koblitzek M, Maly J, Masojidek J, Komenda J, Kucera T, Giardi MT, Mattoo AK, Pilloton R (2002) A biosensor for the detection of triazine and phenylurea herbicides designed using photosystem II coupled to a screen-printed electrode. Biotechnol Bioeng 78:110–116
19. Maly J, Krejci J, Ilie M, Jakubka L, Masojídek J, Pilloton R, Sameh K, Steffan P, Stryhal Z, Sugiura M (2005) Monolayers of photosystem II on gold electrodes with enhanced sensor response–effect of porosity and protein layer arrangement. Anal Bioanal Chem 381(8):1558–1567
20. Bhalla V, Zazubovich V (2011) Self-assembly and sensor response of photosynthetic reaction centers on screen-printed electrodes. Anal Chim Acta 707(1–2):184–190
21. Rouillon R, Tocabens M, Carpentier R (1999) A photoelectrochemical cell for detecting pollutant-induced effects on the activity of immobilized cyanobacterium *Synechococcu*s sp. PCC 7942. Enzyme Microb Technol 25:230–235
22. Giardi MT, Guzzella L, Euzet P, Rouillon R, Esposito D (2005) Detection of herbicide subclasses by an optical multibiosensor based on an array of photosystem II mutants. Environ Sci Technol 39:5378–5384
23. Barthelmebs L, Carpentier R, Rouillon R (2011) Physical and chemical immobilization methods of photosynthetic materials. Methods Mol Biol 684:247–256
24. Shitanda I, Takada K, Sakai Y, Tatsuma T (2005) Compact amperometric algal biosensors for the evaluation of water toxicity. Anal Chim Acta 530:191–197
25. Ringeisen BR, Wu PK, Kim H, Piqué A, Auyeung RYC, Young HD, Chrisey DB, Krizman DB (2002) Picoliter-scale protein microarrays by laser direct write. Biotechnol Prog 18:1126–1129
26. Wu PK, Ringeisen BR, Krizman DB, Frondoza CG, Brooks M, Bubb DM, Auyeung RCY, Pique A, Spargo B, McGill RA, Chrisey DB (2003) Laser manipulation of biomaterials: Matrix-Assisted Pulsed-Laser Evaporation (MAPLE) and MAPLE - Direct Write (MDW). Rev Sci Instrum 74:2546–2557
27. Karaiskou A, Zergioti I, Fotakis C, Kapsetaki M, Kafetzopoulos D (2003) Microfabrication of biomaterials by the sub-ps laser-induced forward transfer process. Appl Surf Sci 245:208–209
28. Serra P, Fernandez Pradas JM, Colina M, Duocastella M, Dominguez J, Morenza JL (2006) Laser-induced forward transfer: a direct-writing technique for biosensors preparation. J Laser Micro Nanoeng 1:236–242
29. Guillemot F, Souquet A, Catros S, Guillotin B, Lopez J, Faucon M, Pippenger B, Bareille R, Rémy M, Bellance S, Chabassier P, Fricain JC, Amédée J (2010) High-throughput laser printing of cells and biomaterials for tissue engineering. Acta Biomater 6:2494–2500
30. Boutopoulos C, Touloupakis E, Pezzotti I, Giardi MT, Zergioti I (2011) Direct laser immobilization of photosynthetic material on screen printed electrodes for amperometric biosensor. Appl Phys Lett 98:093703
31. Porra RJ (2002) The chequered history of the development and use of simultaneous equations for the accurate determination of chlorophylls a and b. Photosynth Res 73:149–156
32. Boutopoulos C, Andreakou P, Kafetzopoulos D, Chatzandroulis S, Zergioti I (2008) Direct laser printing of biotin microarrays on low temperature oxide on Si substrates. Phys Status Solidi A 205:2505–2508
33. Boutopoulos C, Pandis C, Giannakopoulos K, Pissis P, Zergioti I (2010) Polymer/carbon nanotube composite patterns via laser induced forward transfer. Appl Phys Lett 96:041104
34. Deegan R, Bakajin O, Dupont T, Huber G (1997) Capillary flow as the cause of ring stains from dried liquid drops. Nature 389:827–829
35. Duocastella M, Fernández-Pradas JM, Serra P, Morenza JL (2008) Jet formation in the laser forward transfer of liquids. Appl Phys A 93:453–456
36. Deng T, Varanasi KK, Hsu M, Bhate N, Keimel C, Stein J, Blohm M (2009) Nonwetting of impinging droplets on textured surfaces. Appl Phys Lett 94:133109
37. Wakabayashi K, Böger P (2002) Target sites for herbicides: entering the 21st century. Pest Manag Sci 58:1149–1154
38. Maly J, Masojidek J, Masci A, Ilie M, Cianci E, Foglietti V, Vastarella W, Pilloton R (2005) Direct mediatorless electron transport between the monolayer of photosystem II and poly(mercapto-*p*-benzoquinone) modified gold electrode-new design of biosensor for herbicide detection. Biosens Bioelectron 21:923–932
39. Buck RP, Lindner E (1994) Recommendations for nomenclature of ionselective electrodes (IUPAC Recommendations 1994). Pure Appl Chem 66:2527–2536
40. Vittadello M, Gorbunov MY, Mastrogiovanni DT, Wielunski LS, Garfunkel EL, Guerrero F, Kirilovsky D, Sugiura M, Rutherford AW, Safari A, Falkowski PG (2010) Photoelectron generation by photosystem II core complexes tethered to gold surfaces. ChemSusChem 3:471–475
41. Kaniber S, Frolov L, Simmel FC, Holleitner AW, Carmeli C, Carmeli I (2009) Covalently binding the photosystem I to carbon nanotubes. Nano Lett 1:133–134